International Journal of Environment and Geoinformatics (IJEGEO) is an international, multidisciplinary, peer reviewed, open access journal.

Analysis of Different Interpolation Methods for Soil Moisture Mapping Using Field Measurements and Remotely Sensed Data

Mehmet Zeki İmamoğlu and Elif Sertel

Methodology

Radar Image Processing

Radarsat-1 image was rectified using Ground Control Points(GCPs) obtained from ortho-rectified IKONOS imagery of the same region. Different filters were applied to SAR image to suppress the noise effects. Betanought values for every pixel were calculated from back scattered data before relating SAR data and field measurements.

Regression Analysis

Regression analysis was conducted to relate SAR backscattered data with field measurements. In this research, regression analysis with 25 control points with an equation of y = -1,345x + 2,713 has the R^2 value of 0.703, whereas, regression analysis with 15 control points with an equation of y = -1,348x + 2,375 has the R^2 value of 0.832.

Interpolation Methods

Different interpolation and geostatistical techniques were used to create soil moisture map of the study area using point-based field measurements. Firstly, semivariograms were generated using soil moisture value and location of field measurements. Mathematical models like spherical, circular, exponential and Gaussian were fitted to experimental variograms and threshold, range and Nugget variances for each model were examined to find out the best model representing the variograms.

Determination of observed data's experimental variogram structure and forming of theoretical model for its structure are the basis for geostatistical studies (Matheron; 1963; Imamoglu et al.,2011). Regionalized Variable Theory which implements measurements for the spatial dependence of continuous variables, is an important tool in geostatistics and semivariogram is the key in this theory. Variogram represents spatial change of regionalized variables, which are random variables with known location in time and space. Kriging analysis using semivariogram is widely used to estimate parameters in non-sampled locations (Matheron, 1963; Delhomme, 1978; Vieira, 1983).

After the calculation of semivariograms, kriging and co-kriging methods were applied. In addition, deterministic methods of Inverse Distance Weighting (IDW), Global Polynomial Interpolation (GPI), Local Polynomial Interpolation (LPI) and Radial Basis Functions (RBF) were also employed with the aim of producing soil moisture maps.

Inverse Distance Weighting (IDW)

Inverse distance weighting is a deterministic, nonlinear interpolation technique. For soil moisture mapping, IDW uses a weighted average of the soil moisture values from nearby sample points to estimate the soil moisture values of un-sampled locations. IDW is based on the Tobler's first law of geography referring the similarity of two locations decreases with increasing distance [21]. The simplest model involves dividing each of the observations by the distance it is from the target point raised to a power α (Matheron, 1963; Tobler, 1970).

$$z_j = k_j \sum_{i=1}^{n} \frac{1}{d_{ij\alpha}} z_i \qquad (1)$$

The value k_j in this expression is an adjustment to ensure that the weights add up to 1. If the parameter α=1 we have:

$$k_j = \sum_{i=1}^{n} \frac{1}{d_{ij}} \qquad (2)$$

Global Polynomial Interpolation (GPI)

Global Polynomial (GP) is a quick and inexact deterministic interpolator . GP methods give better results for slowly and gradually changing

surfaces. The impacts of the locations toward the edge of the data are higher (Vieira, 1983; Tobler, 1970). There are very few decisions to make regarding model parameters. It is best used for surfaces that change slowly and gradually. However, there is no assessment of prediction errors and it may be too smooth. Locations at the edge of the data can have a large effect on the surface. There are no assumptions required of the data (URL 1). A polynomial that goes through a set number (m+1) of points. A global polynomial is defined over the entire region of space

$$p_m(x) = \sum_{i=0}^{m} c_j x^j \qquad (3)$$

This polynomial is of degree m (highest power is x^m) and order m+1 (m+1 parameters $\{c_j\}$). If we are given a set of m+1 points.

$$y_1 = f_{(x1)}\ , y_2 = f_{(x2)}\ , \ldots y_{m+1} = f_{(x_{m+1})} \qquad (4)$$

Local Polynomial Interpolation (LPI)

LPI is the integration of GP and the moving average procedure. In LPI, 1st, 2nd or 3rd order GP is fitted to local subset of entire data set defined by a window similar to the moving average approach. In order to include sufficient number of data points to the process, the window size should be large. An adjusted version of least squares model by introducing a measure of distance-based weighting called weighted least squares is used in this method for fitting. A power function of distance as a fraction of the window size is used for the calculation of weights. The simplest case of LPI is to apply a circle with redius of R as the moving window. In the below equation, d_i denotes the distance between grid point (x_i, y_i) and a data point (x,y) within the circle an the weight w_i is defined as (Smith et al., 2007).

$$w_i = (1 - \frac{d_i}{R})^P \qquad (5)$$

where p is a user definable power. The least squares procedure then involves minimizing the expression:

$$\sum_{i=1}^{n} w_i (f(x_i, y_i) - z_i)^2 \qquad (6)$$

If p=0 all the weights are 1.

Radial Basis Functions (RBF)

The RBF method is a common approach to interpolate multidimensional scattered data because of being simple and accurately approximating an underlying function (Grady, 2003; Baxter, 1992).

A radial basis function approximation takes the form,

$$s(x) = \sum_{i\epsilon 1}^{n} y_i \varphi(\|x - i\|), \qquad x \epsilon R^d, \qquad (7)$$

Where $\varphi : [0, \infty) \rightarrow R$ is a fixed univariate function and the coefficients $(y_i)_{i \in I}$ are real numbers.

Kriging

Kriging interpolation method estimates values in points with no ground measurements by using variogram structure characteristics of ground samples which are in close proximity with each other. Most important characteristic and advantage of Kriging that separates this method from other interpolation techniques is that there are variance values for the estimation of each and every area or point. This gives information about the confidence degree of the estimated/predicted value (Matheron, 1963; Delhomme, 1978; Sertel et al., 2012).

$$Z(s_0) = \sum_{i=1}^{N} \lambda_i Z(S_i) \qquad (8)$$

where:

$Z(s_i)$ = the measured value at the ith location, λ_i = an un1978known weight for the measured value at the ith location, λ_i = an unknown weight for the measured value at the ith location, s_0 = the prediction location, N = the number of measured values.

Cokriging:

Cokriging is a variation of the ordinary kriging which takes into account a secondary variable having relationship with the main variable that you want to estimate. This method minimizes the variance of the estimation error by exploiting the cross-correlation between two variables. Cross-correlated information contained in the secondary variable resulted in decrease of the variance of the estimation errors. Application of cokriging is useful if the primary variable of interest is under sampled and secondary variable is more denser to provide the cross correlated information (Laurent et al., 2013; Xiaoqing et al., 2013). Soil moisture is used as primary variable due to the limited number of field measurements and SAR backscattering which includes the signal of soil moisture and much more denser considering the size and spatial resolution of SAR image is used as secondary variable in our research.

The Cokriging estimation model can be summarized as follows:

$$Z(x_0) = \sum_{i=1}^{n} \omega_{1i} Z_1(x_i) + \sum_{i=1}^{p} \omega_{2j} Z_2(x_j) \quad (9)$$

where $Z(x_0)$ is the position of the sample point; ω_{1i} and ω_{2j} are two regionalized variables; and $Z_1(x_i)$ and $Z_2(x_j)$ are weight coefficients (Eldeiry and Garcia, 2010).

In this study; 11 points, which approximately correspond to %20 of 36 sample points are chosen as ICPs to to check the accuracy of each method applied. At the first experiment, 25 CPs were used for different interpolation approaches and RMSE values were obtained for each model and then RMSE of 11 CPs were also analyzed to illustrate the accuracy of each mode. As a second step, 10 CPs were omitted and another experiment was conducted with remaining 15 CPs to analyze the impact of number and distribution of CPs on different interpolation approaches. Same 11 ICPs were used to analyze the accuracy of the second experiment to be consistent for both data set.

Results and Discussion

First of all, Radarsat-1 imagery was geometrically corrected then betanought values are calculated by using pixel's reflection values. Regression analysis was performed between this betanouht values and soil moisture values of samples collected from the ground in order to reveal the correlation among them. Figure 2 shows the regression analysis with 25 control points, R^2 is found 0.703 in this application. Later, 10 additional control points (homogenously selected) excluded from the model and regression analysis is performed with 15 control points. Figure 3 shows the correlation between Radarsat-1 betaught values and 15 control points. This model's R^2 is rises to 0.832.

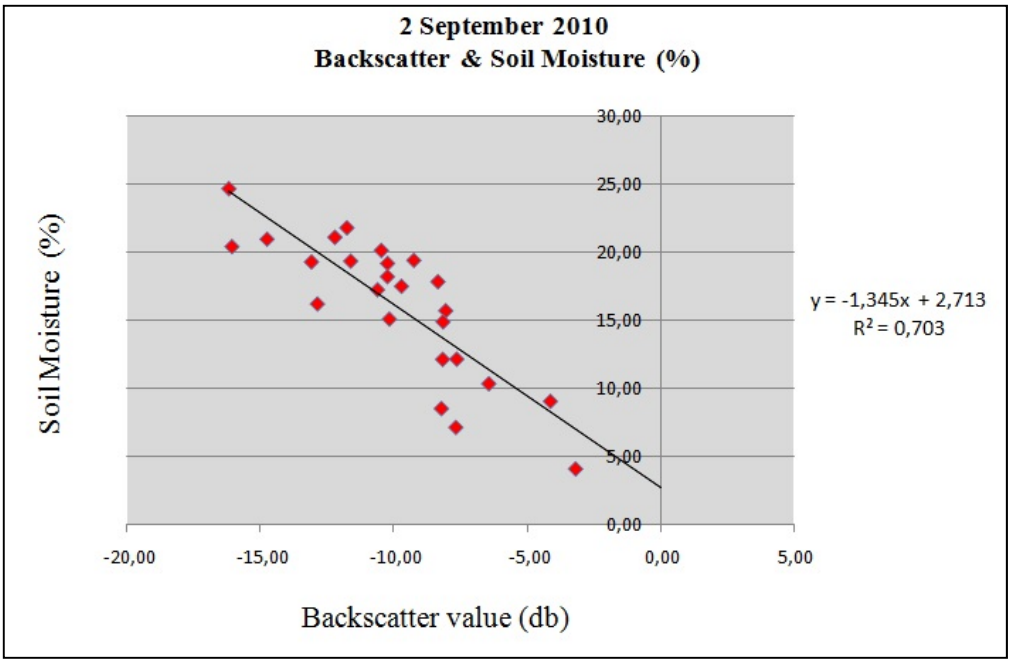

Figure 2. The Correlation Between Radarsat-1 Backscatter Values and Soil Moisture Value of 25 Control Points.

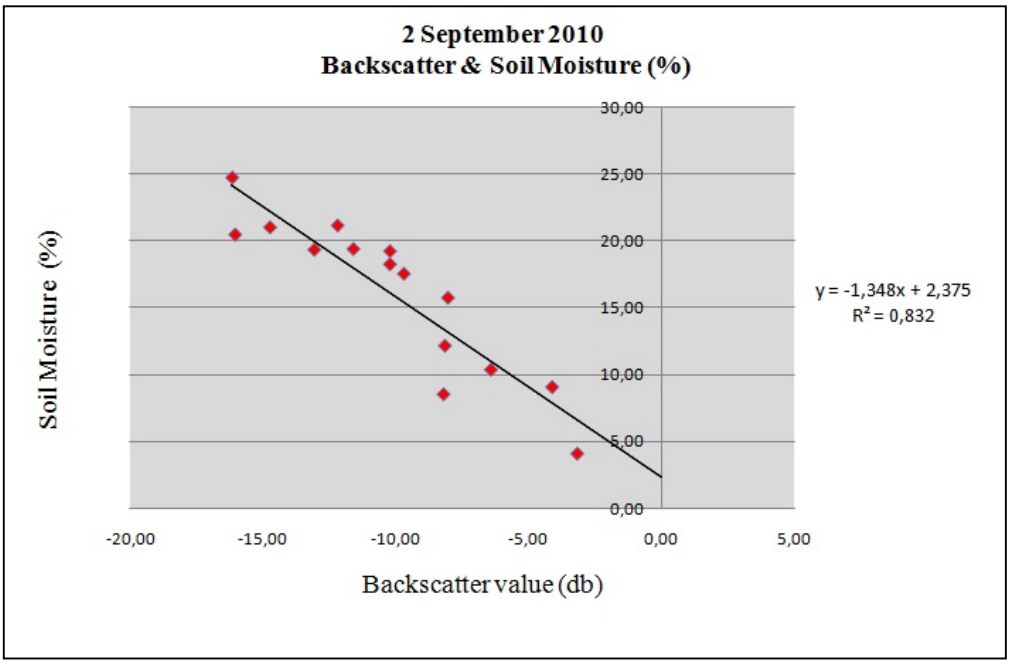

Figure 3. The Correlation Between Radarsat-1 Backscatter Values and Soil Moisture Value of 15 Control Points

Secondly, 11 points which are roughly %20 of the ground control points are selected as check points and various analyses are performed using 25 control points. At first, regression analyses and different interpolation techniques are executed with this points. In last stage, 11 check point values are compared with these results with the purpose of finding the best performing analyses. Also, 10 more control points are excluded from these models to find out the effects of the number of control points on results by analyzing remaining 15 points and comparing the results with 11 check points.

Figure 4 presents soil moisture maps interpolated using 25 CPs using Inverse Distance Weighting (IDW), Global Polynominal Interpolation (GPI), Local Polynominal Interpolation (LPI), Radial Basis Functions (RBF), Kiriging and Cokriging methods. A general pattern similarity can be noticed in these maps created with different methods. Furthermore, it is seen that southwest and north east of the maps shows higher soil moisture values while middle regions have less soil moisture.

Figure 5 shows the maps created from 15 control points with different methods, which exhibit great similarity with 25 control point maps. Again, southwest and northeast of the maps shows higher values of soil moisture then the middle regions.

Tables 1-3 are created to summarize and compare the results achieved by different methods. In these tables, the locations of 11 check points, moisture values measured in these locations, land use information, results of different interpolation techniques and the difference of these results are presented.

Table 1 presents the moisture values of 11 check points calculated from 25 control points and the respected techniques used for analyses. Examination of RMS values presented at table 3 in conjunction with ground control soil moisture values and results of the interpolation techniques shows that best performing method is Ordinary Kriging with RMS = 3,534. However, individual examination of points shows that other methods have better results in some points. For example, at 1st check point, IDW has better results. Similarly GPI in 2nd check point, LPI in 3rd check point, Ordinary Kriging in 4th check point gives better results. Nevertheless, results acquired by Radar data and Cokriging method applied to Radar data have the highest error and lowest performance.

Table 2 shows the soil moisture values of 11 check points obtained from maps created by the interpolation of 15 points with different techniques. Examining the RMS values in table 3 in conjunction with ground sample values and map values shows that best performing result for this model is obtained through Cokriging with RMS=3,935. Similar to the 25 point analysis, at some individual points, other methods gives better results such as RDF for 1st point, GPI for 2nd point, LPI for 3rd point, Kriging for 8th point and Kokriging for 11th point gives better results.

Conclusions and Further Research

In this study, soil moisture maps were created using various interpolation techniques and geostatistical methods by means of field soil moisture and SAR image data. Alternative methods have the advantage of being faster in wider study areas over the conventional methods. It is observed that having accurate results with interpolation techniques depend on the frequency of sampling locations. More accurate results could be obtained by increasing the number of control points which are homogenously distributed over the study area. Sampling of the ground truth also affects the accuracy of the border between soil groups. If the physical parameters such as depth of soil, slope of the terrain are taken into consideration, different interpolation and geostatistical methods could give better results. In this study, Inverse Distance Weighting (IDW), Global Polynominal Interpolation (GPI), Local Polynominal Interpolation (LPI), Radial Basis Functions (RBF) interpolation techniques and Kriging, Cokriging geostatistical techniques are compared and Ordinary Kriging is discovered to be the best performer among them

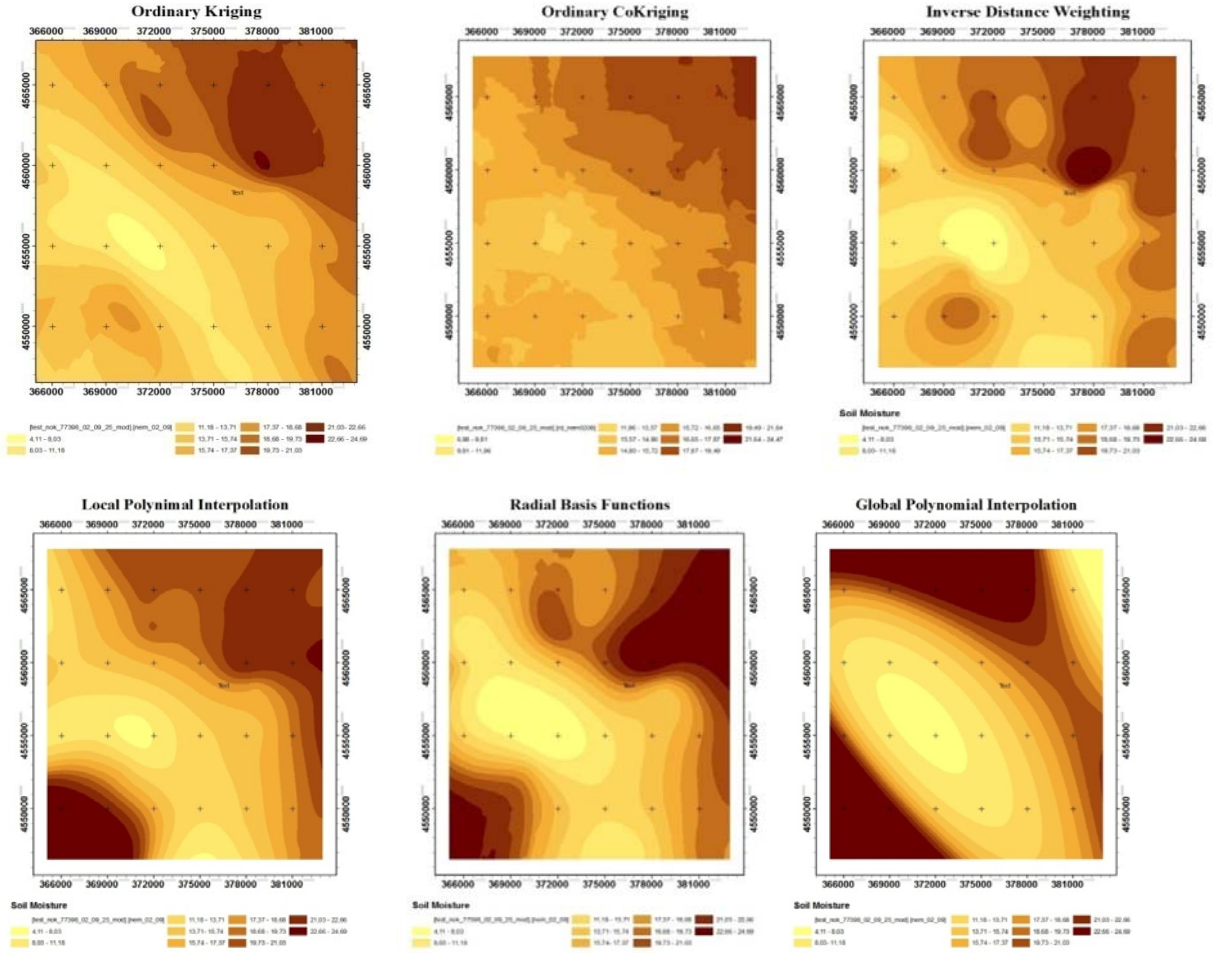

Figure 4. Soil Moisture Maps Calculated From 25 Soil Moisture Value Control Points With Different of Interpolation Techniques

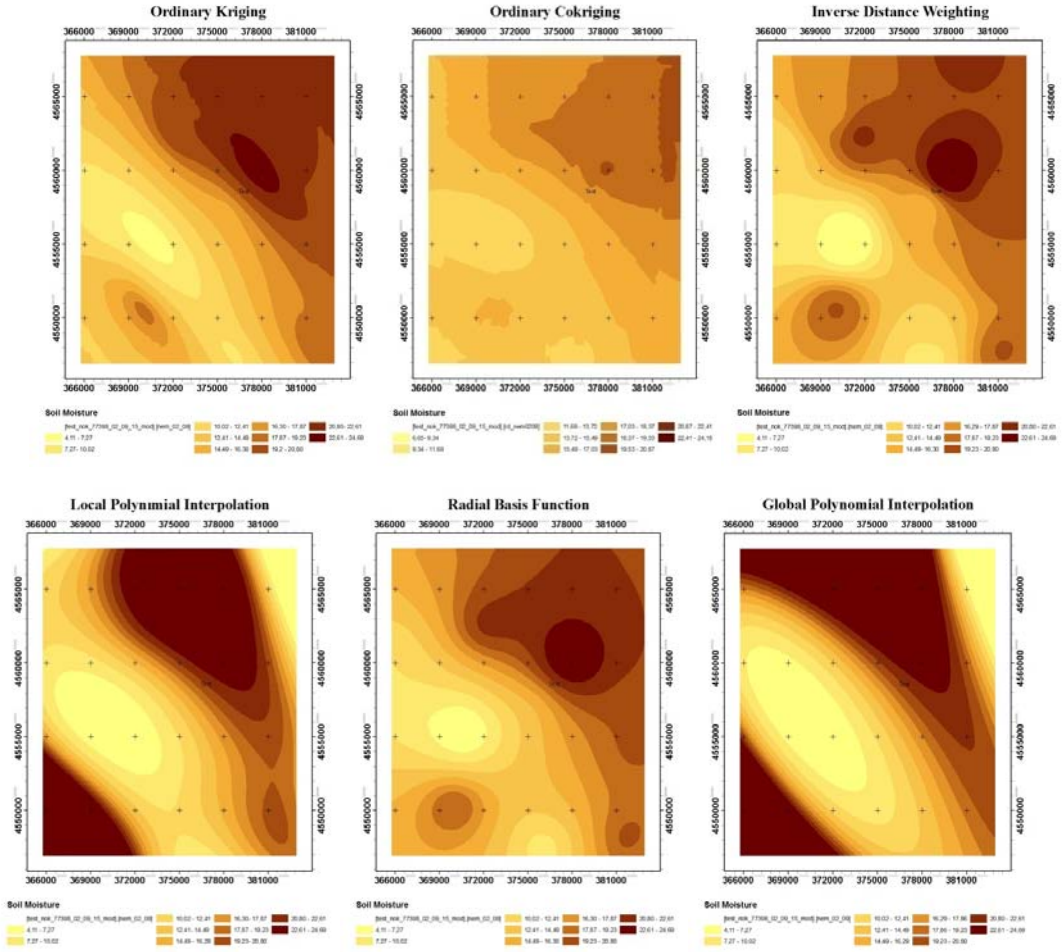

Figure 5. Soil Moisture Maps Calculated From 25 Soil Moisture Value Control Points With Different of Interpolation Techniques

Table 1. Soil Moisture Values of 11 check points obtained from maps created by the interpolation of 25 Control Points With Different Techniques

S.No.	Sample points	x	y	Measured	Kriging	Measured-Kriging	Cokriging	Measured-Cokriging	Radar	Measured-Radar	IDW	Measured-IDW	GPI_3	Measured-GPI	LPI	Measured-LPI	RBF	Measured-RBF
1	101/2	376146,23	4547454,43	7,99000	9,63284	-1,64284	13,68590	-5,69590	17,71661	-9,72661	9,07000	-1,08000	12,62410	-4,63410	9,24333	-1,25333	9,07144	-1,08144
2	103	374191,12	4550257,45	8,54000	11,09720	-2,55720	14,79320	-6,25320	23,56334	-15,02334	12,37570	-3,83570	9,85620	-1,31620	12,39760	-3,85760	12,00580	-3,46580
3	104	372843,33	4552194,738	12,53000	9,98316	2,54684	14,53040	-2,00040	6,07515	6,45485	11,15250	1,37750	8,29683	4,23317	11,93080	0,59920	10,83600	1,69400
4	110	369258,89	4557157,38	7,84521	8,20485	-0,35964	13,95250	-6,10729	20,36789	-12,52268	8,84601	-1,00080	7,17290	0,67231	9,96888	-2,12367	5,11640	2,72881
5	111	369122,92	4559992,17	8,20641	11,98030	-3,77389	15,45500	-7,24859	14,43001	-6,22360	14,77640	-6,56999	8,82022	-0,61381	14,49940	-6,29299	10,42360	-2,21719
6	118	371327,87	4559720,80	11,83602	14,63550	-2,79948	15,70120	-3,86518	19,49514	-7,65912	17,31270	-5,47668	10,20670	1,62932	15,36870	-3,53268	13,74380	-1,90778
7	124	382489,91	4555136,34	24,40778	18,99370	5,41408	17,48030	6,92748	12,51518	11,89260	18,80860	5,59918	20,56570	3,84208	21,11410	3,29368	20,44790	3,95988
8	126	382829,83	4551622,91	23,86602	18,61920	5,24682	16,11990	7,74612	16,14404	7,72198	18,56320	5,30282	21,10450	2,76152	20,61490	3,25112	20,20750	3,65852
9	137	376235,86	4549542,23	9,67291	12,02710	-2,35419	14,76530	-5,09239	16,38947	-6,71656	12,15000	-2,47709	10,67040	-0,99749	12,01750	-2,34459	12,12360	-2,45069
10	139	365800,60	4558418,77	18,36267	19,36670	-1,00403	17,19800	1,16467	10,89059	7,47208	15,56250	2,80017	19,59050	-1,22783	18,72190	-0,35923	17,31200	1,05067
11	140	370229,35	4552593,38	18,39706	15,13600	3,26106	14,87550	3,52156	13,69858	4,69848	16,19270	2,20436	11,26470	7,13236	14,72180	3,67526	16,00030	2,39676

Table 2. Soil Moisture Values of 11 check points obtained from maps created by the interpolation of 15 Control Points With Different Techniques

S.No.	Sample points	x	y	Measured	Kriging	Measured-Kriging	Cokriging	Measured-Cokriging	Radar	Measured-Radar	IDW	Measured-IDW	GPI_3	Measured-GPI	LPI	Measured-LPI	RBF	Measured-RBF
1	101/2	376146,23	4547454,43	7,99000	9,07540	-1,08540	12,71600	-4,72600	17,41207	-9,42207	9,07000	-1,08000	12,00560	-4,01560	9,28135	-1,29135	9,07083	-1,08083
2	103	374191,12	4550257,45	8,54000	10,45780	-1,91780	14,43290	-5,89290	23,27185	-14,73185	12,64980	-4,10980	8,46468	0,07532	9,80965	-1,26965	13,37000	-4,83000
3	104	372843,33	4552194,738	12,53000	9,27309	3,25691	14,34860	-1,81860	5,74465	6,78535	13,47750	-0,94750	6,28980	6,24020	7,51949	5,01051	13,10640	-0,57640
4	110	369258,89	4557157,38	7,84521	7,15905	0,68616	13,08340	-5,23819	20,06927	-12,22406	8,24904	-0,40383	3,84544	3,99977	4,11298	3,73223	7,73605	0,10916
5	111	369122,92	4559992,17	8,20641	11,81230	-3,60589	15,14090	-6,93449	14,11816	-5,91175	14,31760	-6,11119	6,45153	1,75488	9,01956	-0,81315	12,82430	-4,61789
6	118	371327,87	4559720,80	11,83602	14,68790	-2,85188	15,63640	-3,80038	19,19457	-7,35855	17,00550	-5,16948	9,97227	1,86375	11,80280	0,03322	15,06230	-3,22628
7	124	382489,91	4555136,34	24,40778	19,91410	4,49368	17,69130	6,71648	12,19904	12,20874	19,19270	5,21508	19,40520	5,00258	18,37800	6,02978	19,53550	4,87228
8	126	382829,83	4551622,91	23,86602	18,53250	5,33352	16,91340	6,95262	15,83600	8,03002	18,53220	5,33382	20,17240	3,69362	17,72640	6,13962	18,92300	4,94302
9	137	376235,86	4549542,23	9,67291	12,06520	-2,39229	14,36700	-4,69409	16,08198	-6,40907	12,14990	-2,47699	10,22330	-0,55039	11,68140	-2,00849	12,16310	-2,49019
10	139	365800,60	4558418,77	18,36267	22,45160	-4,08893	18,74120	-0,37853	10,57083	7,79184	21,53490	-3,17223	22,99910	-4,63643	23,06170	-4,69903	21,97670	-3,61403
11	140	370229,35	4552593,38	18,39706	11,99450	6,40256	14,16640	4,23066	13,38508	5,01198	14,18400	4,21306	8,81526	9,58180	9,86406	8,53300	12,89700	5,50006

Table 3. RMS Values Crated by 25 and 15 Control Points With different Techniques

Methods	25 Points	15 Points
	RMS	RMS
Kriging	3,53400	4,25000
Cokriging	3,59600	3,93500
IDW	3,80200	4,75800
GPI	4,65200	5,98100
LPI	3,69400	
RBF	3,70500	4,66900

But, other techniques did give better results in some individual points. However, RMS error matrices of mentioned techniques revealed that the lowest RMS error is acquired by Ordinary Kriging in 25 point model, Cokriging in 15 point model. Inspection of Table 1 and Table 2 shows that higher control points yield optimum results and lower RMS values. IDW, RBF and LPI methods produce similar results wiith ordinary kriging.

SAR-based results produce comperatively coearser RMSE values compared to other interpolation methods due to the impact on C-band on soil moisture. On land cover classes having barren land and sparse vegetation SAR data provides good results wehereas on densely vegetated ares C-band SAR fails to simulate soil moisture precisely. Moreover, it is importnat to emphasize the betetr results obtained with co-kriging compared to regresiion while creating soil moistore maps from SAR images in conjuction with field soil moisture measurement.

Our results show the importance of ICPs usage for validation of diiffernt approach. In some cases, althous RMSE of CPs used to fit model produce reasonable results, validation of these results with ICPs which were not used in modeling procedure illustrates that RMSE value can vary.

Acknowledgements

The authors would like to thank Istanbul University for laboratory analysis, Istanbul Technical University-Center of Satellite Communication and Remote Sensing (ITU-CSCRS) for RADRSAT-1 image support, Istanbul Metropolitan Municipality for providing some spatial data used in the research and Ms. Irmak YAY ALGAN for her kind contributions

References

Algan, O., Yalçın, M.N., Özdoğan, M., Yılmaz, Y., Sarı, E., Kırcı-Elmas, E., Yılmaz,İ., Bulkan,Ö., Ongan, D., Gazioğlu, C., Nazik, A., Polat, M.A., and Meriç, E. (2011). Holocene coastal change in the ancient harbor of Yenikapı–İstanbul and its impact on cultural history. Quaternary Research, Vol .76 (1), pp.30-45.

Alpar, B., Burak, S. and Gazioğlu, C. (1997). Effect of weather system on the regime of sea level variations in İzmir Bay, Turkish Journal of Marine Sciences, 3 (1997), pp. 83–92

Alvarez-Mozos,J., Casalí, J., González-Audícana, M., Verhoest N. E. C., 2006. Assessment of the Operational Applicability of RADARSAT-1 Data for Surface Soil Moisture Estimation. IEEE Transactions on Geoscience and Remote Sensing 44, 913-924.

Baghdadi, N. Aubert, M. Cerdan, O., Franchistéguy, L., Viel, C., Martin, E., Zribi, M., Desprats, J.F. 2007. Operational Mapping of Soil Moisture Using Synthetic Aperture Radar Data: Application to the Touch Basin (France), Sensor.

Baxter, B. J.C. 1992. The Interpolation Theory Of Radial Basis Functions.

Beven, K.J.; Fisher, J. 1996. Remote sensing and scaling in hydrology. In Scaling up hydrology using remote sensing; Stewart, J.B., Engman, E.T., Fedes, R.A., Kerr, Y., Eds.; Wiley Press: Chichester, UK.

Brocca, L., Moramarco, T., Melone, F., Wagner, W., Hasenauer, S., Hahn, S., 2012. Assimilation of surface- and root-zone ASCAT soil moisture products intorainfall—runoff modeling. IEEE Trans. Geosci. Remote Sens., 2542–2555.

Delhomme, J.P.,1978. Kriging in the Hydrosciences, Advances in Water Resources, 5, 251-266.

Eldeiry AA, Garcia LA 2010. Comparison of ordinary kriging, regression kriging, and cokriging techniques to estimate soil salinity using LANDSAT images. J.Irrig Drain ASCE 136: 355–364.

Gazioğlu, C. Burak, S.Z., Alpar, B., Türker, A. and Barut I.F. 2010 Foreseeable impacts of sea level rise on the southern coast of the Marmara Sea (Turkey), Water Policy 12 (6), 932-943

Gevaerta, A.I. Parinussab, R.M. Renzulloc, L.J. Dijkd, A.I.J.M. V., and Jeu. R.A.M. D. 2016. Spatio-temporal evaluation of resolution enhancement for passivemicrowave soil moisture and vegetation optical depth. International Journal of Applied Earth Observation and Geoinformation 45 (2016) 235–244.

Grady B. Wright 2003. Radial Basis Function Interpolation, Numerical and Analytical Developments. Imamoglu,M.Z., Sertel, E., Kurucu,Y., Örmeci, C., 2011. Mapping Of Different Soil Proporties By Means Of Geostatistical Methods and Analysis With GIS, II. Soil and Water Supply Congress, 2011, Ankara, Turkey.

Hejmenowska, B. And Mularz, S. 2000. Integratıon of multitemporal Ers Sar And Landsat TM data for soil moisture assesment, IAPRS, Vol, XXXIII, Amsterdam.

IPCC, 2013. Summary for Policymakers. In: Climate Change 2013: The Physical Science Basis. Contribution of Working Group I to the Fifth Assessment Report.

Jaroslaw Kaya Zawadzki, Mateusz K˛edzior, 2016. Soil moisture variability over Odra watershed: Comparison betweenSMOS and GLDAS data. International Journal of Applied Earth Observation and Geoinformation 45 (2016) 110–124

Kaya., H. and Gazioğlu, C. 2015. Real Estate Development at Landslides, International Journal of Environment and Geoinformatics Vol:2(1), 62-71.

Laiolo, P., et al., 2015. Impact of different satellite soil moisture products on the predictions of a continuous distributed hydrological model. Int. J. Appl. EarthObserv. Geoinf.

Laurent L, Boucard P, Soulier B. 2013. Generation of a cokriging metamodel using a multiparametric strategy. Comput Mech 51: 151–169.

M.J.Smith, M.F.Goodchild, P.A.Longley, 2007, Geospatial Analysis: Comprehensive Guide to Principles, Techniques and Software Tools.

Matheron G. 1963. Principles of geostatistics. Econ Geol 58:1246–1266.

Musaoglu, N., Kaya, S., Seker, D. Z., & Goksel, C. (2002). A case study of using Remote Sensing Data and GIS for Land Management, Catalca Region. FLG XXII International Congress USA, Washington D.C. USA, April 19-26, 2002.

Olea, R.A. 1982. Optimization of the High Plains Aquifer Observation Network, Kansas. Kansas Geological Survey, Grandwater Series, No. 7, Lawrence, - Kansas.

Panegrossi, G., Ferretti, R., Pulvirenti, L., Pierdicca, N., 2011. Impact of ASAR soilmoisture data on the MM5 precipitation forecast for the Tanaro flood event ofApril 2009. Nat. Hazards Earth Syst. Sci. 11, 3135–3149.

Qiang Wang, Rogier van der Velde, Zhongbo Su, Jun Wen 2016. Aquarius L-band scatterometer and radiometer observations over aTibetan Plateau site. International Journal of Applied Earth Observation and Geoinformation 45 (2016) 165–177

Şeker, D.Z., Direk, Ş., Musaoğlu, N. and Gazioğlu, C. 2013. Determination of Effects of Coastal Deformation Caused by Waves and Storms at Black Sea Coast of Turkey

utilizing InSAR Technique, AGU Fall Meeting Abstracts, Vol. 1, 1629

Seneviratne, S.I., Corti, T., Davin, E.L., Hirschi, M., Jaeger, E.B., Lehner, I., Orlowsky,B., Teuling, A.J. 2010. Investigating soil moisture-climate interactions in achanging climate: a review. Earth-Sci. Rev. 99, 125–161.

Sertel E, Demirel H and Kaya Ş, 2012. Predictive Mapping Air Pollutantas: A Spatial Approach, Proceedings CD of the Fifth International Spatial Data Quality Symposium, ITC, CD Nm.17, Enschede, Netherland.

Sertel E, Kutoglu SH and Kaya Ş. 2007. Geometric correction accuracy of different satellite sensor images: application of figure condition. Int J Remote Sens 28(20):4685–4692. doi:10.1080/01431160701592452

Simav, Ö.; Şeker, D.Z. and Gazioğlu, C. 2013. Coastal inundation due to sea level rise and extreme sea state and its potential impacts: Çukurova delta case. Turk. J. Earth Sci., 22, 671–680.

Tobler, W. 1970. A Computer Movie Simulating Urban Growth in the Detroit Region. Economic Geography, 46(2): 234-240.

URL 1: http://pro.arcgis.com/en/pro-app/help/analysis/geostatistical-analyst/how-global-polynomial-interpolation-works.htm.

Vieira, S.R., Hatfield, J.L., Nielsen, D.R., Biggar, J.W., 1983. Geoistatistical Theory and Application to Variabilitiy of Some Agronomical Properties, Hilgardia, 51, 3, 1-75.

Western, A.W. and Blöschl, G., 1999. On the spatial scaling of soil moisture, Journal of Hydrology, 217: 203-224.

Xiaoqing Z, Miao L, Shuying Z 2013. Spatial Interpolation of the Chlorophyll-a Concentration in Zhalong Wetland Based on Cokringing. Chin.Agric.Sci.Bull 29: 160–164.